(Article begins on next page)

Behaviour at the peritoneal interface of next-generation prosthetic materials for hernia repair

Gemma Pascual[1,3,4], Selma Benito-Martínez[2,3,4], Marta Rodríguez[2,3,4], Bárbara Pérez-Köhler[1,3,], Francisca García-Moreno[2,3,4], Juan M. Bellón[2,3,4]

[1]Department of Medicine and Medical Specialties, Faculty of Medicine and Health Sciences, University of Alcala, Madrid, Spain
[2] Department of Surgery, Medical and Social Sciences, Faculty of Medicine and Health Sciences, University of Alcala, Madrid, Spain
[3] Networking Biomedical Research Centre on Bioengineering, Biomaterials and Nanomedicine (CIBER-BBN), Madrid, Spain
[4] Ramon y Cajal Health Research Institute (IRYCIS), Madrid, Spain

Abstract

Background When using a prosthetic material in hernia repair, the behaviour of the mesh at the peritoneal interface is especially important for implant success. Biomaterials developed for their intraperitoneal placement are known as composites and are made up of two different-structure materials, one is responsible for good integration within host tissue and the other is responsible to make contact with the viscera. This study examines the behaviour at the peritoneal level of two composites, the fully degradable Phasix-ST® and the partially degradable Symbotex®. A polypropylene mesh (Optilene®) served as control. **Methods** Sequential laparoscopy from 3 to 90 days, in a preclinical model in the New Zealand white rabbit, allowed monitoring adhesion formation. Morphological studies were performed to analyse the neoperitoneum formed in the repair process. Total macrophages were identified by immunohistochemical labelling. To identify the different macrophage phenotypes, complementary DNAs were amplified by qRT-PCR using specific primers for M1 (TNF-α/CXCL9) and M2 (MRC1/IL-10) macrophages.

Results The percentage of firm and integrated adhesions remained very high in the control group over time. Both composites showed a significant decrease in adhesions at all study times and in qualitative terms were mainly loose. Significant differences were also observed from 7 days onwards between the two composites, increasing the values in Phasix over time. Neoperitoneum thickness for Phasix was significantly greater than those of the other meshes, showing mature and organized neoformed connective tissue.

Immunohistochemically, a significantly higher percentage of macrophages was observed in Symbotex. mRNA expression levels for the M2 repair-type macrophages were highest for Phasix but significant differences only emerged for IL-10. **Conclusions** Fewer adhesions formed to the Symbotex than Phasix implants. Ninety days after implant, total macrophage counts were significantly higher for Symbotex, yet Phasix showed the greater expression of M2 markers related to the tissue repair process.

Keywords Hernia repair · Peritoneal interface · Composites · Sequential laparoscopy · Adhesion formation · Neoperitoneum · Macrophage response

When using a prosthetic material in hernia repair, the behaviour of the mesh at the peritoneal interface is especially important for implant success. Laparoscopic intraperitoneal onlay mesh (IPOM) technique requires that the prosthetic mesh is placed in direct contact with the visceral peritoneum.

Continuing research efforts have sought to find a material showing optimal behaviour at all interfaces created between the implant and host tissue. Such optimal behaviour consists of a good balance between the drawbacks of adhesion formation and the benefits of adequate host tissue incorporation, providing strength to the repair zone. However, to date, this ideal prosthetic material does not exist [1].

The material most used today is the reticular mesh polypropylene. Both preclinical and clinical studies have confirmed its good behaviour at the extraperitoneal interface, that is, when placed outside the peritoneal cavity [2, 3]. When a polypropylene mesh, however, needs to make contact with the visceral peritoneum, adverse effects can arise such as adhesions, intestinal obstruction [4], implant migration to hollow organs [5], or more serious complications like intestinal fistula [6–8].

Today's biomaterials developed for their intraperitoneal placement are known as *composites* [9] and are made up of two different-structure materials. One of these materials is responsible for good integration within host tissue and the other implant surface is designed to make contact with the viscera within the abdominal cavity [10]. These composite designs have evolved over time and presently their polymer contents have partially or even totally been replaced with a biodegradable component. A prerequisite for the use of these prosthetic meshes is that they induce the formation of a good mesothelial cell coating at the peritoneal interface. Effectively, the adequate deposition of these cells is the key to successful repair [11].

The present study was designed to experimentally examine the behaviour at the peritoneal level of two composites, the fully degradable Phasix-ST® and the partially degradable Symbotex®. A lightweight polypropylene mesh served as a control (Optilene®). This behaviour was followed by sequential laparoscopy allowing observation of the implant in the short term and also avoiding excessive use of experimental animals. Our study focuses on monitoring adhesion formation and was complemented with an analysis of the neoperitoneum formed on the mesh implant in the repair process. Special attention was paid to the foreign body reaction induced by the materials at such a critical level as the

peritoneal interface. The main population analysed was that of macrophages, which play an essential role in the response to a foreign body, as is a hernia repair mesh. These macrophages feature a wide phenotypic spectrum ranging from proinflammatory (M1) to antiinflammatory and tissue remodelling (M2) phenotypes. M1 macrophages support acute inflammation and defence against microorganisms and macromolecular foreign bodies. In large measure, they are phagocytic and secrete proinflammatory cytokines such as IL-1b, IL-6, IL-12, IL-23, CXCL and TNF-α [12, 13]. In contrast, M2 macrophages mitigate acute inflammation promoting repair, tissue remodelling and fibrosis with a regulator antiinflammatory phenotype. These macrophages are also highly phagocytic and produce extracellular matrix components and angiogenic factors. M2 macrophages have been attributed a role in increasing the expression of several markers such as arginase 1, Ym1, FIZZ1, CD163, CD206, MHC-II, TGM2, IL-10, TGF-β and IL-1ra [12, 14].

While the initial notion was that macrophages were mainly involved in the non-desired degradation and rejection of biomaterials, it is now clear that they are needed for the adequate integration within host tissue of non-degradable biomaterials, and for the degradation and substitution of degradable biomaterials [12]. This means that the delicate balance between proinflammatory and antiinflammatory macrophages can be influenced by biomaterial structure or additional treatments to elicit the functional remodelling of tissue rather than prolonged inflammation, fibrosis and healing [15, 16].

Materials and methods

Experimental animals

Eighteen male New Zealand White rabbits of mean weight 3000 g were used. As it was a preclinical research that was not involving human subjects, informed consent was not required.

The study was conducted in accordance with the Guide for the Care and Use of Laboratory Animals of the National and European Institutes of Health (Spanish law 06/2013, Spanish Royal Decree 53/2013, European Directive 2010/63/EU and European Convention of the Council of Europe ETS123). All procedures were performed at the Animal Research Centre of Alcalá University (Madrid, Spain), which is registered with the Directorate General for Agriculture of the Ministry of Economy and Technology Innovation of the Community of Madrid (ES280050001165), indicating that all facilities legally covered the needs and requirements of this research. The study protocol was approved by the Committee on the Ethics of Animal Experiments of the University of Alcalá.

Prosthetic materials

The meshes used were (Fig. 1A) as follows:

- Optilene Mesh Elastic® (*Opt*): a lightweight, monofilament, non-absorbable polypropylene mesh (B. Braun, Barcelona, Spain).
- Phasix-ST® (*Phax*): a monofilament resorbable scaffold composed of poly-4-hydroxybutyrate with a resorbable hydrogel coating (Bard, Warwick, USA).
- Symbotex® (*Sym*): a composite mesh composed of a non-absorbable polyester monofilament and a bioabsorbable collagen film (Medtronic, Minneapolis, USA).

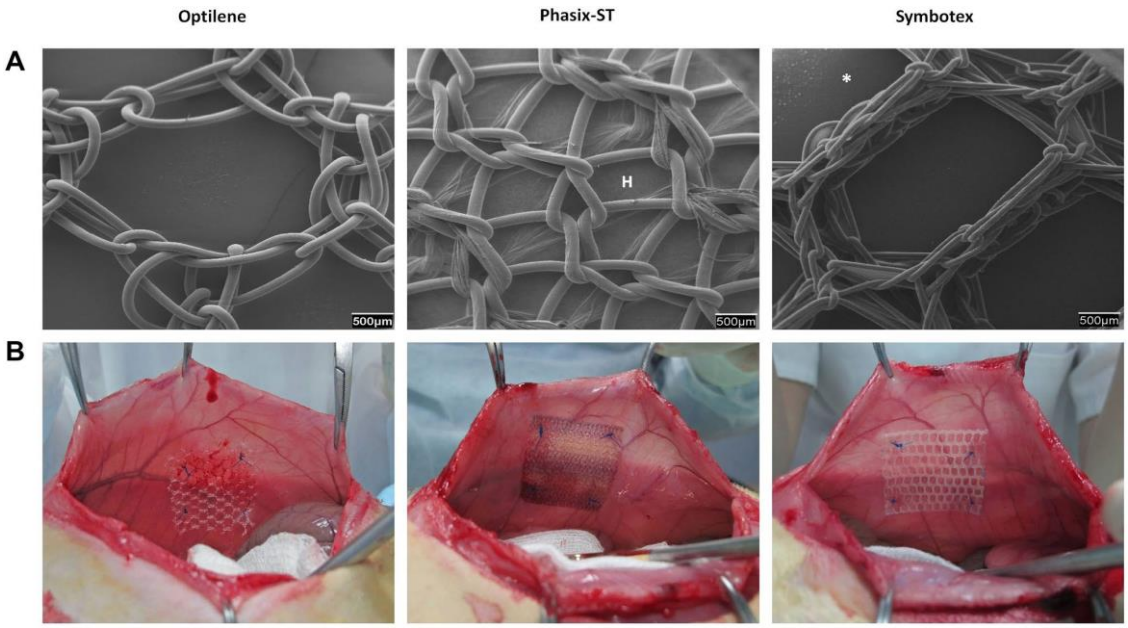

Fig. 1 **A** Characterization of the prosthetic materials. Scanning electron microscopy (SEM) images (× 20). Absorbable hydrogel coating (H) and collagen bioabsorbable film (*). **B** Surgical technique and macroscopic appearance of the meshes after implant. All three meshes, Optilene, Phasix-ST, and Symbotex were fixed onto the parietal peritoneum using four stitches

Surgical technique

Eighteen rabbits were anaesthetized with a mixture of ketamine (20 mg/kg, Imalgene, Merial, Spain) and xylazine (3 mg/kg, Xilagesic 2%, Calier, Spain) administered intramuscularly. Preoperatively and once daily for the first 3 days postsurgery, animals were given analgesia (0.05 mg/ kg buprenorphine, Buprecare, Divasa Farmavic, Spain).

Using a sterile surgical technique, a longitudinal incision about 6-cm long was made along the midline. On the left side of the laparotomy and 1 cm from the linea alba, a prosthetic patch (3 × 3 cm) was placed on the intact parietal peritoneum and fixed at the implant corners by placing four individual 4/0 polypropylene stitches (Fig. 1B). When fragments of each of the prosthetic materials were implanted on the parietal peritoneum, we checked carefully the mesh was placed in the right place and it was smooth without rolled edges. The abdominal wall was closed using a running 3/0 polypropylene suture, while the skin was closed by simple interrupted stitches of 3/0 silk suture.

Animals were randomized to receive one of the prosthetic materials making a total of six implants per biomaterial.

Adhesion formation

To quantify adhesions between the visceral peritoneum and the implants, on days 3, 7 and 14 postimplant, each animal was anaesthetized and examined laparoscopically.

Laparoscopy was performed under general anaesthesia by introducing a 3 mm, 0° laparoscope (Karl Storz, Tuttlingen, Germany) into the peritoneal cavity through a metal trocar (Karl Storz). Access was gained through the linea alba 1 cm from the lower limit of the laparotomy incision. To aid observations, the abdominal cavity was filled with CO_2 at a maximum pressure of 8 mm of Hg. Once the examination was completed, the laparoscopy equipment was removed and the skin closed.

Observations were video recorded for subsequent review. At each follow-up time, the surface areas of the meshes covered with adhesions were measured. This was done by tracing the outlines of the adhesions on transparent polyethylene templates of the same size as the implants using the photographs taken during the laparoscopic study.

At 90 days postimplant, the animals were sedated with up to 20 mg/kg of xylazine (Rompun; Bayer, Leverkusen, Germany) and then euthanized with a lethal dose of 20% sodium pentobarbital (Dolethal, Vetoquinol SA, Lure, France). Photographs were taken and adhesions assessed in each animal as previously described. Implants and adhesions were collected for subsequent studies (morphology, immunohistochemistry and real-time PCR (qRT-PCR).

Adhesion outlines were transferred to a digital template of the mesh surface, producing an image that was analysed using Image J (NIH, USA; http://image j.nih.gov/ij). Adhesions were assessed and classified according to their macroscopic characteristics as follows: loose (transparent and easily dissected), firm (denser adhesions, whitish in colour and difficult to dissect) or integrated (within the prosthesis/ visceral peritoneum interface and difficult to dissect away from the biomaterial and intestinal serosa) [17].

Results were expressed as the percentage implant surface covered by adhesions (range, 0–100%; from no adhesions to completely covered). The intraabdominal structure involved, omentum or intestine, location of adhesions and surface appearance of the implant were noted.

Morphological analysis

Standard fixation procedures were used for both microscopy techniques. For light microscopy, samples were fixed in F13 solution and embedded in paraffin. Tissue blocks were cut into 5 µm sections and placed onto slides coated with polylysine (SIGMA, Merk, USA). Finally, the sections were hydrated and stained with haematoxylin eosin and Masson's trichrome (Goldner-Gabe). Samples were examined under a light microscope Zeiss Axiophot (Zeiss, Germany).

For scanning electron microscopy (SEM), samples were fixed with 3% glutaraldehyde, dehydrated and mounted on stubs using double-sided tape. Critical point was reached in a critical point dryer (E-3000; Polaron, United Kingdom) with carbon dioxide. Samples were then metalized with gold palladium and examined in a Zeiss scanning electron microscope (DSM-950; Carl Zeiss, Oberkochen, Germany).

Postimplant neoperitoneal thicknesses

On 10 histologic sections (in × 5 microscopy fields) per group, we measured the thickness of the neoperitoneum formed over each intraperitoneal mesh. We defined neoperitoneal thickness as the distance between the prosthetic material and the neoformed mesothelium. Images for analysis were captured using a digital camera fitted to a light microscope (Axiocam HR; Zeiss).

Macrophage response

Immunohistochemistry

Macrophages were identified by immunohistochemical labelling with the monoclonal antibody to rabbit macrophages RAM 11 (DAKO M-633, USA). This antibody reacts with a cytoplasmic antigen in rabbit macrophages, as a result, this marker identifies the total macrophage population. Paraffin sections were hydrated and incubated with primary antibody RAM 11 overnight, after blocking unspecific binding with bovine serum albumin (SIGMA). For antibody detection, the avidin–biotin alkaline-phosphatase staining method was used. A chromogenic substrate containing naphthol phosphate and fast red was used to develop the positive reaction. Cell nuclei were counterstained with acid haematoxylin.

Labelled macrophages were determined on tissue sections by performing counts in 10 microscopy fields (magnification × 200) per sample captured by a digital camera fitted to a Zeiss Axiophot light microscope (Carl Zeiss, Oberkochen, Germany) and analysed with Image J (https ://image j.nih. gov/ij/). Results were expressed as mean positive cell percentages of the total number of cell nuclei per section.

RNA isolation and real-time PCR (qRT-PCR)

Implant fragments (with incorporated host tissue) were obtained for qRT-PCR analysis and stored at − 80 °C until use. RNA was extracted using guanidine-phenol–chloroform isothiocyanate procedures with TRIzol (Invitrogen, Carlsbad, CA, USA) and recovered from the aqueous phase by precipitation. RNA amounts and purity were measured at optical wavelengths of 260/280 nm and 260/230 nm in a NanoDrop ND-1000 spectrophotometer (Thermo Fisher Scientific Inc., DE, USA).

Complementary DNA was synthesized from 200 ng of total RNA by reverse transcription using oligo dT primers (Amersham, Fairfield, USA) and the M-MLV reverse transcriptase enzyme (Invitrogen).

To identify the different macrophage phenotypes (M1 and M2), complementary DNAs were amplified using specific primers for M1 macrophages: chemokine C-X-C motif ligand 9 (CXCL9) (sense 5′- CAG GAC TCC ATT CCA CCA CT -3′ and antisense 5′- GGA CTT CCT TGA ACT CCA ATC A -3′) and tumour necrosis factor alpha (TNF-α) (sense 5′-CTC CTA CCC GAA CAA GGT CA -3′ and antisense 5′-CGG TCA CCC TTC TCC AAC T-3′); or for M2 macrophages: mannose receptor C-Type 1 (MRC1, CD206) (sense 5′- TGA TGG GAC CCC TGT AAC CT-3′ and antisense 5′- TGC CCA GTA TCC ATC CTT GC-3′) and human Interleukin-10 (IL-10) (sense 5′- GAA CTC CCT GGG GGA AAA C -3′ and antisense 5′- GGC TTT GTA GAC GCC TTC CT -3′). The housekeeping gene glyceraldehyde 3-phosphate dehydrogenase **(**GAPDH**)** (sense 5′-TCA CCA TCT TCC AGG AGC GA-3′ and antisense 5′-CAC AAT GCC GAA GTG GTC GT-3′) was used as an internal control.

RT-PCR was performed in a StepOnePlus real-time PCR system (Applied Biosystems, Foster City, California, USA). The samples were analysed in triplicate and gene expression was normalized against the expression value recorded for the constitutive gene GAPDH.

Statistical analysis

Data are provided as mean ± standard error of the mean and compared between pairs of groups using the Mann–Whitney U test. All statistical tests were performed using the package GraphPad Prism 5.0 for Windows (GraphPad Software Inc., La Jolla, CA, USA). Significance was set at $p < 0.05$.

Results

Macroscopic observations

No signs of infection or implant rejection were observed throughout the study in any of the animals.

Sequential laparoscopy

- 3 days postimplant

  In the control *Opt* implants, firm adhesions appeared 3 days after surgery. In contrast, adhesions to *Phax* and *Sym* were classified as loose (Fig. 2).

  Adhesion percentages covering the implants were higher for *Opt* than the other materials, reaching values of 65.12% of the implant surface versus 7.75% and 2.84% for *Phax* and *Sym*, respectively, differences being significant in relation to *Opt* (Fig. 3).

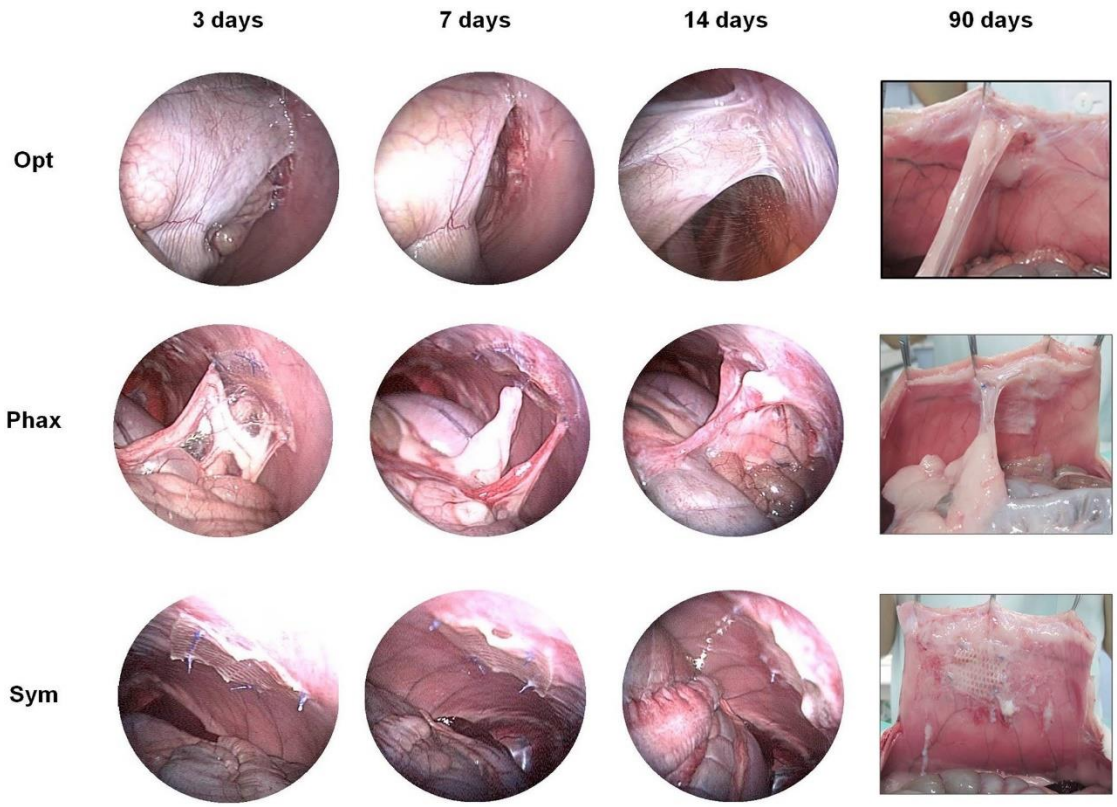

Fig. 2 Sequential laparoscopic images of adhesions formed to the different meshes 3, 7, 14 and 90 days after implant

– 7 days postimplant

Adhesions were firm in the *Opt* group and some firm adhesions to *Phax* started to appear. The *Sym* prosthesis maintained its minimal amounts of loose adhesions (Fig. 2).

Between days 3 and 7, adhesion percentages stabilized in *Opt* (72.55%) and *Phax* (5.90%), maintaining a significant difference between each other. In the case of *Sym,* adhesion percentages fell (0.37%) and the difference was significant versus the other two study groups (Fig. 3).

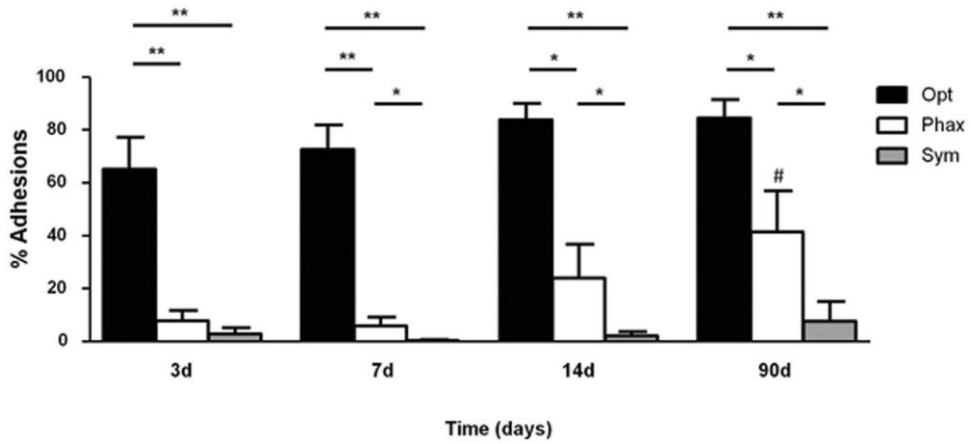

Fig. 3 Percentage mesh areas covered by adhesions in each study group at the different follow-up times. Optilene mesh showed the highest adhesion percentage at all time points with differences being significant with respect to the other meshes. Mann–Whitney U test: *$p < 0.05$, **$p < 0.01$, $^{\#}p < 0.05$ versus *Phax* at 7 days

– 14 days postimplant

In qualitative terms, adhesion types remained the same as at the earlier time point for the three prosthetic materials (Fig. 2).

Percentage adhesions were still significantly higher for *Opt* (83.78%) than the other two implants. The *Phax* mesh showed a greater adhesion percentage than at the earlier time points (23.95%), but differences were not significant. The *Sym* implant surface was most free of adhesions (2.04%), remaining stable over time and differing significantly compared with *Phax* (Fig. 3).

– 90 days postimplant

Adhesions were classed as integrated and firm for *Opt,* alternating between firm and loose for Phax, and continued to be loose for *Sym* (Fig. 2).

At this time point, adhesion percentages remained stable in *Opt* (84.60%), and increased significantly from the percentages recorded at 7 days in *Phax* (41.44%). The significant differences observed at the previous time point were maintained. Adhesions to the *Sym* implants were slightly increased (7.55%) albeit non-significantly with respect to prior time points (Fig. 3).

In every implant, most adhesions appeared mainly at the borders of the mesh, in the areas of polypropylene sutures that anchored the mesh to the abdominal wall.

Morphological study

At 90 days, the prostheses of the different study groups *Opt*, *Phax* and *Sym* appeared integrated within a connective repair tissue, the neoperitoneum, of different characteristics depending on the prosthetic material. In general, this newly formed tissue was deposited around and in between the mesh filaments. Small blood vessels could be seen in the filament interstices of the different materials, along with fibroblasts and inflammatory cells, mostly monocytes, macrophages and giant foreign body cells (Fig. 4).

In the case of the *Opt* implants, the neoperitoneum formed a thin layer in the zones free of adhesions. This neoformed connective tissue was loose, disorganized and featured a greater adipose compartment than the remaining groups. On the *Phax* implants, this layer was significantly thicker and more uniform across the mesh surface. Further, the connective tissue was well collagenized giving rise to a mature neoperitoneum. The hydrogel was almost completely reabsorbed such that only small remnants could be seen in isolated zones of the tissue. At this time point, the synthetic filaments showed no signs of their reabsorption. In contrast, the collagen film on the *Sym* mesh appeared fully reabsorbed. In this group, the neoperitoneum showed an even thickness, although the repair tissue was not too structured and tissue discontinuities were observed, which could correspond to zones where the film had been absorbed.

Scanning electron micrographs (Fig. 4) of the intraperitoneal interface of the implants allowed for assessment of the extent of mesothelialization produced on each one. The *Sym* prosthesis showed a mesothelial coating that lined the repair tissue formed between the prosthetic filaments and pores. Mesothelial cells showed a polygonal morphology, numerous apical microvilli and were arranged forming a mosaic monolayer characteristic of this cell type. *Phax* showed similar behaviour, although in these implants we observed slight loss of cohesion between mesothelial cells in zones coinciding with the protrusion of filaments towards the peritoneal-facing surface. In contrast, the intraperitoneal surface of the Opt implants was coated by a fibrous-looking tissue with scarce dispersed oval-shaped mesothelial cells. Adhesion tissue remains could also be seen (Fig. 4)

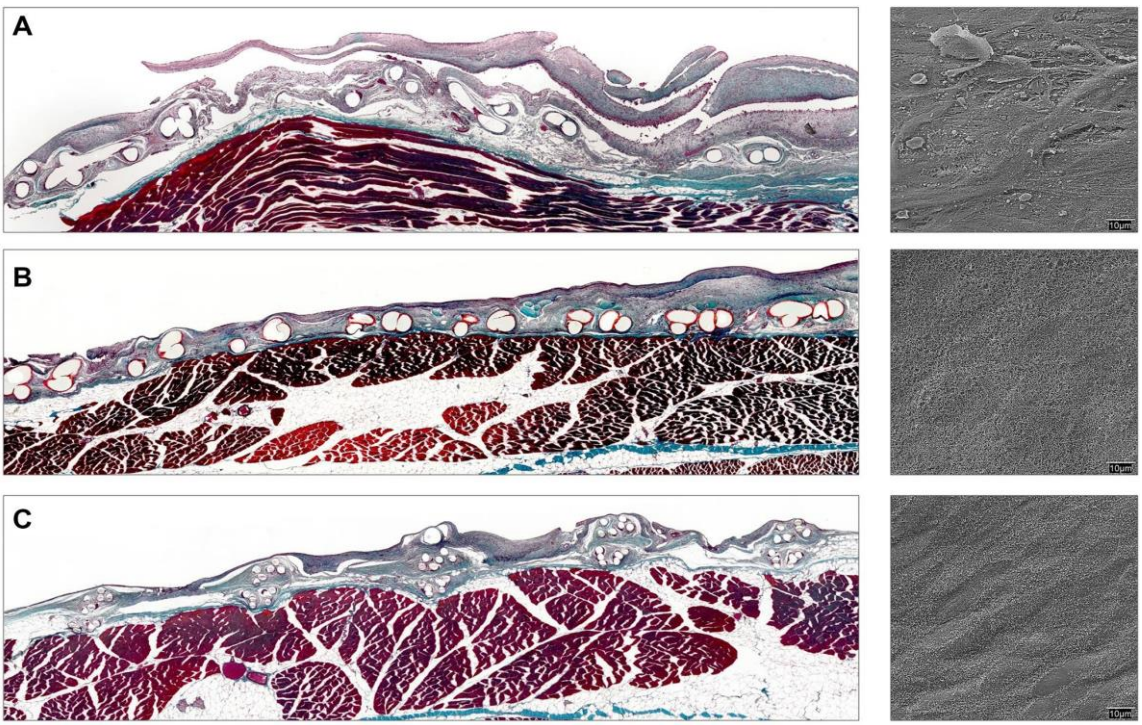

Fig. 4 Composition of the implants (Masson's trichrome, × 50, left panel) and scanning electron micrographs of their surface (× 1000, rightpanel) at 90 days postimplant A Optilene, B Phasix-ST, C Symbotex

Neoperitoneal thickness

Neoperitoneal thicknesses in the three mesh groups varied significantly (Fig. 5).

Thicknesses for *Phax* were significantly greater (287.4 ± 33.83 µm) than those of the non-degradable meshes (*Opt* 57.66 ± 12.54 µm, *Sym*, 120.0 ± 21.53 µm) ($p < 0.001$). Neoperitoneal thickness differences between *Opt* and *Sym* were also significant ($p < 0.05$).

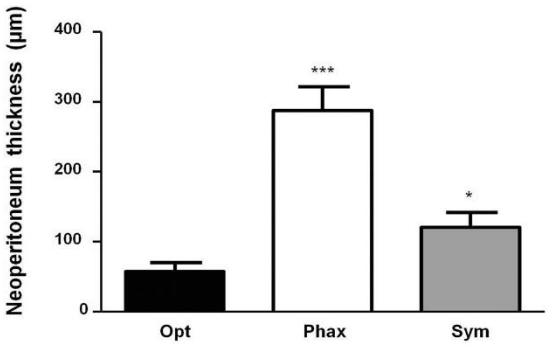

Fig. 5 Mean neoperitoneum thicknesses recorded in each study group 90 days after implant. Mann–Whitney U test: ***$p < 0.001$ versus Optilene and Symbotex, *$p < 0.05$ versus Optilene

Macrophage response

Immunohistochemistry

On the three implant types, RAM 11-positive cells were mainly detected around the prosthetic filaments, especially in the form of giant foreign body reaction cells. Isolated labelled cells could also be seen in the neoformed connective tissue that occupied the zones between the filaments of the prosthetic materials (Fig. 6A).

In our quantitative analysis of labelling, a significantly higher percentage of macrophages was observed ($p < 0.05$) in the *Sym* than *Opt* and *Phax* groups. Thus, macrophage percentages were somewhat more reduced for the *Phax* mesh, though differences with respect to *Opt* were not significant (Fig. 6B).

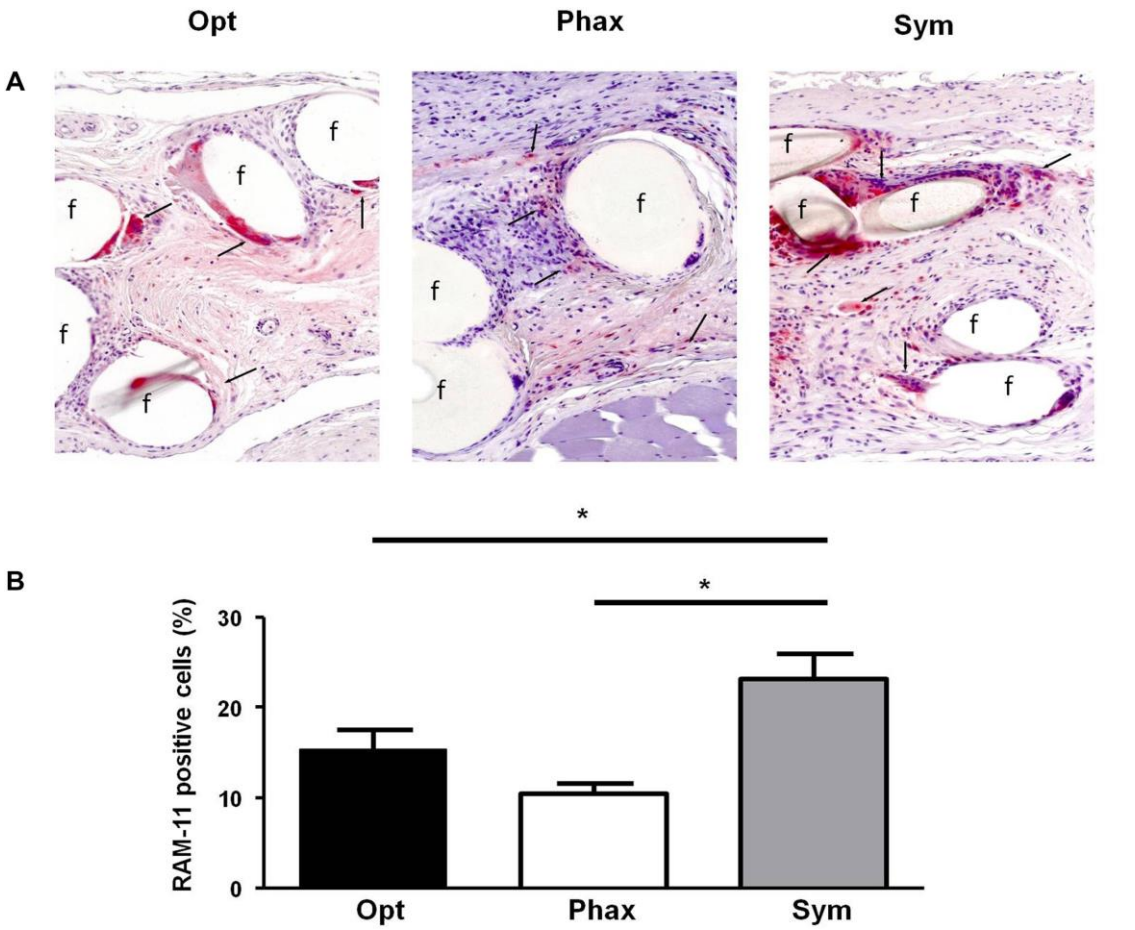

Fig. 6 **A** Immunohistochemical labelling of rabbit macrophages using the RAM 11 monoclonal antibody (× 200) 90 days after implant. f: mesh filaments. → : labelled macrophages. **B** Percentage positive cells recorded for each study group at 90 days postimplant. Results expressed as the mean ± standard error of the mean. Phasix-ST showed the lower percentage of RAM-11-positive cells. Mann–Whitney U test: *$p < 0.05$

qRT-PCR

All three study groups showed similar expression levels of mRNA for CXCL9, a marker of M1 proinflammatory macrophages. Expression levels of TNF-α mRNA were lowest for *Sym* though differences were not significant versus *Phax* and *Opt* (Fig. 7A).

Messenger RNA expression levels for the different M2 repair-type macrophages (MRC1 and IL-10) were highest for *Phax* but significant differences only emerged for IL-10 mRNA between *Phax* and *Opt* ($p < 0.05$). (Fig. 7B).

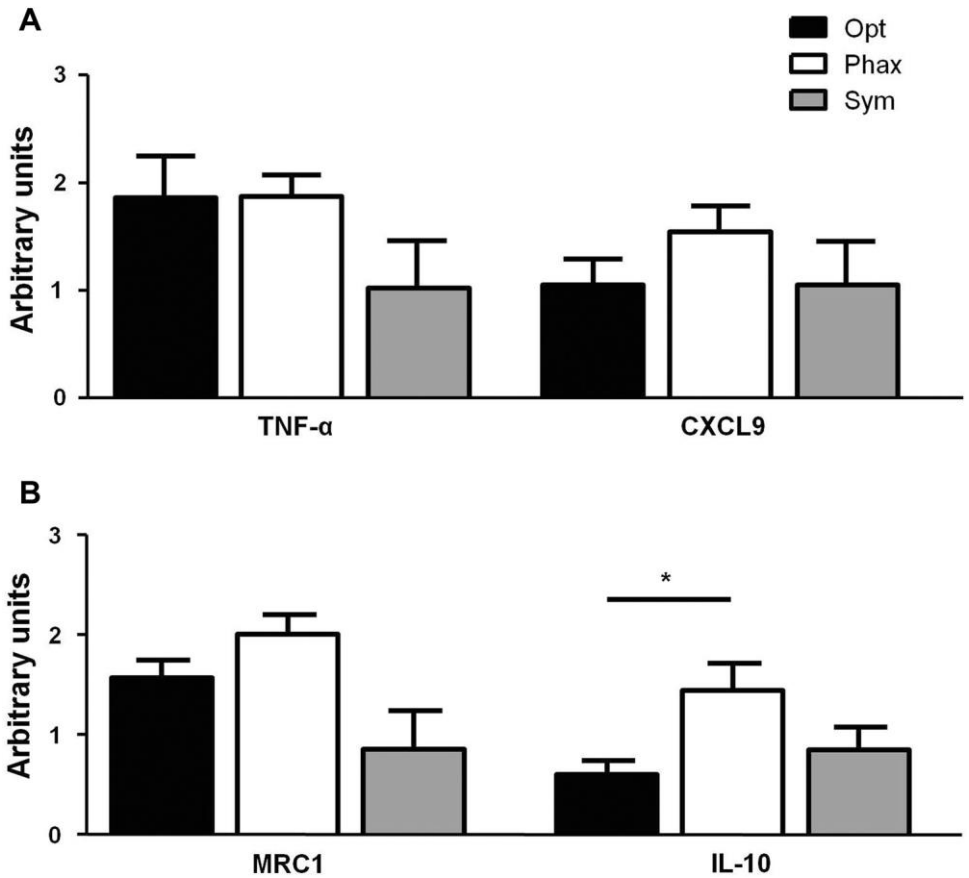

Fig. 7 Relative mRNA levels determined by qRT-PCR in the implant areas. A TNF-α and CXCL9 (M1 macrophage markers) mRNA levels, B MRC1 and IL-10 (M2 macrophage markers) mRNA levels. Gene expression was normalized to expression recorded for the reference gene GAPDH. MannWhitney U test: *p < 0.05

Discussion

It is well known that porous meshes of the polypropylene/ polyester type generate an interface, when the mesh is placed in contact with the visceral peritoneum, where the most common complication is adhesion formation. This has led to the development of double-layered prosthetic materials called composites [18, 19]. Initially, the peritoneal side of these materials was non-absorbable. Subsequently, materials were introduced whose peritoneal surface had the property of being absorbable [20–22], to create an adequate peritoneal interface with the visceral contents of the peritoneal cavity. This interface needs to be conducive to host mesothelial cell deposition, a behaviour conferred by a biomaterial that has a smooth surface, facilitating good cell expansion and giving rise to an uninterrupted cell monolayer [11].

Delayed mesothelial cell deposition on a prosthetic material might explain the more frequent appearance of adhesions, as occurs with reticular type prostheses (e.g. polypropylene). On the other hand, rapid mesothelial deposition improves the peritoneal interface. Other authors have also reported that the presence of mesothelial cells and early neoperitoneal formation are crucial to prevent adhesions during peritoneal recovery following surgical insult [23]. The mesothelial cell monolayer itself seems to have certain properties that avoid adhesion formation. Mesothelial cell membranes contain large amounts of phospholipids, especially phosphatidylcholine. These membranes are thought to act as a lubricant avoiding the appearance of fibrin deposits [24]. Notwithstanding, sometimes these deposits do form because of a precarious fibrinolytic capacity of mesothelial cells. Hence, they may be colonized by fibroblasts giving rise to adhesions [25]. Moreover, any form of mechanical damage could cause discontinuity in the peritoneal layer.

In our study, the control polypropylene mesh showed the greater adhesion formation. In contrast, the interface formed by *Phax* and especially by *Sym* was practically adhesion-free at each study time point.

Adhesions to the materials examined here appeared early and were already visible 3 days after implant. Their formation, nevertheless, could have commenced before this period [20, 26] and continued up to 7 days postsurgery. Beyond this interval, adhesiogenesis did not proceed and laparoscopic observations at 7 and 14 days were similar. In the longer term, there could be more adhesions to some implants. This was effectively observed in the case of *Phax* but not the other biomaterials. Possibly, the peritoneal surface of this mesh is not sufficiently smooth to elicit the formation of an adequate mesothelial layer. SEM studies have shown that 2 weeks after peritoneal damage and the application of an adhesion barrier, the injured surface was covered with different amounts of fibres and mesothelial cells, depending on the barrier used [27].

In clinical studies [28–31] in which, following the implant of a composite prosthesis, there was a need for revision surgery for another reason, minimal

adhesion formation was observed to a prosthetic material of similar design to *Sym.*

Adhesions to polypropylene implants are the consequence of inappropriate mesothelialization of the implant surface. The reticular mesh structure does not elicit the genesis of a mesothelial cell monolayer. In the case of a macroporous polypropylene mesh, this interface can be improved by the interposition of epiplon between the mesh and visceral peritoneum [32, 33]. In clinical practice, this manoeuvre has yielded good results including a lack of fistula-like complications. Interposition of the peritoneal hernia sac itself has also led to good outcomes [34]. Both epiplon and the peritoneal sac are rich in mesothelial cells and thus promote the mesothelialization of the biomaterial.

Consistent with the findings of others [35], when a prosthetic material is placed in contact with the peritoneal viscera, the general design of composite materials does not avoid adhesion formation rather it quantitatively minimizes this event. Adhesions affecting our *Phax* and *Sym* implants coincided with fixation zones to the parietal peritoneum.

Other preclinical studies have examined the peritoneal healing process following the implant of a composite mesh (polyglecaprone 25-coated polypropylene) designed to minimize adhesions, observing complete coverage by the neoperitoneum at 7 days postimplant and minimal adhesion formation continuing until 28 days postimplant [23].

In response to the tissue injury produced by the implant of a biomaterial, macrophages are recruited and depending on the specific characteristics of the material, they will determine the type and intensity of the host response [36, 37]. Some studies have shown how the physical properties of a biomaterial, including its stiffness, pore size, surface topography and chemistry, will induce the different in vitro polarization behaviour of macrophages [36, 38]. Other studies have shown that in an in vitro inflammatory environment, macrophages still react in a biomaterial-dependent manner [39]. It is this essential role of macrophages in wound healing including the repair of tissues with biomaterial support that prompted our interest in investigating the response of this cell population to different biomaterials.

Our morphological observations revealed that the resorbable mesh *Phax* elicited the formation of a thick neoperitoneum along with a mature good-quality neoformed tissue. This could be related to a diminished inflammatory reaction as our immunohistochemical analysis using the RAM 11 antibody revealed a reduced macrophage response in this group. Compared to the other biomaterials examined, the advance of the repair process in this group corresponded to a greater expression of M2 macrophages, as determined through qPCR, which in the case of IL-10 was significant compared to observations in the PP group. Although this particularity appears not to be a great development in the surgical

practice, at the clinical level, this benefit in the progress of tissue remodelling is a very important factor in the acquisition of mechanical capabilities of the tissue.

Our findings for *Phax* are in agreement with those of other authors [40–42] who detected a moderate inflammatory reaction around mesh filaments. Although there is some controversy over the host tissue response to degradable materials, most investigators also propose that the polarization of M1 macrophages towards M2 macrophages is beneficial in terms of tissue generation and restructuring [12]. *Phax* also has the benefit that is a completely reabsorbable mesh. This material is degraded via slow enzymatic degradation until 18 months postimplant, and eventually it completely vanishes from the recipient organism after being replaced with a good-quality repair tissue at the implant site. In contrast, in the other two groups of implants, the prosthetic material will remain in the implant zone for ever.

Quantitatively, the greater overall macrophage response was elicited by the *Sym* mesh, the difference being significant in relation to the other two biomaterials. This high macrophage response could be attributed to reabsorption of the collagen film this type of prosthesis has on its peritoneal surface. This film will condition the repair process by giving rise to a less mature, less organized connective tissue and a significantly thinner neoperitoneum compared with the *Phax* implant. Our analysis of the M2 macrophage phenotype revealed that despite being the material eliciting the greater overall macrophage response, *Sym* showed considerably reduced gene expression of M2 cell population markers. This means that in the repair process, the predominant macrophages were of an inflammatory phenotype.

In a preclinical study [23] addressing the use of a composite mesh (polyglecaprone 25-coated polypropylene), the authors observed the early formation of a neoperitoneum (at 7 days) integrated within the underlying composite mesh that matured between 14 and 21 days. Thus, observations at 28 days were a mature peritoneum consisting of remodelled fibrous tissue with no foreign body granuloma present.

The *Opt* mesh showed the least organization and thickness of the neoperitoneum. These findings are similar to those of others [43] who described the build up of macrophages around the prosthetic filaments with numbers decreasing the further from these sites. We observed the significantly lower expression of the M2 marker IL-10 in comparison with *Phax*, supporting the idea that non-absorbable reticular meshes induce a proinflammatory situation.

With regard to the relationship between adhesion formation and macrophage phenotype, Hong et al. [44] reported inverse correlation between adhesion formation and M2 marker expression (arginine 1 and MRC1). However, no association was found with other markers of this phenotype such as IL-10 and IL-4. Our results differ from these findings as our *Sym* implants showed low MRC1 marker expression but also a lower percentage of adhesions. However,

the other M2 marker examined, IL-10, showed an increasing trend compared to the polypropylene meshes.

The limitations of this preclinical study are mainly related to the animal model used although some of its findings match those detected in human clinical practice, especially observations in the intraperitoneal polypropylene implants. Another limitation of the study is that results are promising but still are not sufficient to indicate the type of mesh used in the hernia repair.

In conclusion, our findings indicate that: (a) fewer adhesions formed to the *Sym* than *Phax* implants; (b) 90 days after implant, macrophage counts were significantly higher for *Sym*, yet *Phax* showed the greater expression of M2 macrophages related to the tissue repair process.

Funding The study was supported by Grant “SAF2017-89481-P” from the Spanish Ministry of Economy and Competitiveness.

Compliance with ethical standards

Disclosures Drs. Gemma Pascual, Selma Benito-Martínez, Marta Rodríguez, Bárbara Pérez-Köhler, Francisca García-Moreno and Juan M. Bellón have no conflicts of interest or financial ties to disclose.

References

1. Klinge U, Park JK, Klosterhalfen B (2013) The ideal mesh? Pathobiology 80:169–175
2. Cassar K, Munro A (2002) Surgical treatment of incisional hernia. Br J Surg 89(5):534–545
3. Pascual G, Rodriguez M, Gomez-Gil V, García-Honduvilla N, Buján J, Bellón JM (2008) Early tissue incorporation and collagen deposition in lightweight polypropylene meshes: bioassay in an experimental model of ventral hernia. Surgery 144(3):427–435
4. Yilmaz I, Karakas DO, Sucullu I, Ozdemir Y, Yucel E (2013) A rare cause of mechanical bowel obstruction: mesh migration. Hernia 17(2):267–269
5. Aziz F, Zaeem M (2014) Chronic abdominal pain secondary to mesh erosion into ceacum following incisional hernia repair: a case report and literature review. J Clin Med Res 6(2):153–155
6. Ott V, Groebli Y, Schneider R (2005) Late intestinal fistula formation after incisional hernia using intraperitoneal mesh. Hernia 9(1):103–104
7. Moussi A, Daldoul S, Bourguiba B, Othmani D, Zaouche A (2012) Gas gangrene of the abdominal wall due to late-onset enteric fistula after polyester mesh repair of an incisional hernia. Hernia 16(2):215–217

8. Arnold MR, Kao AM, Otero J, Marx JE, Augenstein VA, Sing RF, Colavita PD, Kercher K, Henniford BT (2020) Mesh fistula after ventral hernia repair: what is the optimal management? Surgery 167(3):590–597
9. Amid PK (1997) Classification of biomaterials and their related complications in abdominal wall hernia surgery. Hernia 1:5–8
10. Deeken CR, Faucher KM, Matthews BD (2012) A review of the composition, characteristics, and effectiveness of barrier mesh prostheses utilized for laparoscopic ventral hernia repair. Surg
Endosc 26(2):566–575
11. Bellón JM, García-Honduvilla N, López R, Corrales C, Jurado F, Buján J (2003) In vitro mesothelialization of prosthetic materials designed for the repair of abdominal wall defects. J Mater Sci Mater Med 14(4):359–364
12. Klopfleisch R (2016) Macrophage reaction against biomaterials in the mouse model—phenotypes, functions and markers. Acta Biomater 43:3–13
13. Cohen HB, Mosser DM (2013) Extrinsic and intrinsic control of macrophage inflammatory responses. J Leukoc Biol 94(5):913–919
14. Roszer T (2015) Understanding the mysterious M2 macrophage through activation markers and effector mechanisms. Mediators Inflamm. https ://doi.org/10.1155/2015/81646 0
15. Badylak SF, Valentin JE, Ravindra AK, McCabe GP, StewartAkers AM (2008) Macrophage phenotype as a determinant of biologic scaffold remodelling. Tissue Eng A 14(11):1835–1842
16. Brown BN, Sicari BM, Badylak SF (2014) Rethinking regenerative medicine: a macrophage-centered approach. Front Immunol 5:510
17. Bellon JM, Contreras LA, Bujan J, Jurado F (1996) Effect of phosphatidylcholine on the process of peritoneal adhesion following implantation of a polypropylene mesh prosthesis. Biomaterials 17(14):1369–1372
18. Walker AP, Henderson J, Condon RE (1993) Double-layer prostheses for repair of abdominal wall defects in a rabbit model. J Surg Res 55(1):32–37
19. Amid PK, Shulman AG, Lichtenstein IL, Sostrin S, Young J, Hakakha M (1994) Experimental evaluation of a new composite mesh with the selective property of incorporation to the abdominal wall without adhering to the intestines. J Biomed Mater Res 28(3):373–375
20. Baptista ML, Bonsack ME, Delaney JP (2000) Seprafilm reduces adhesions to polypropylene mesh. Surgery 128(1):86–92
21. Szabo A, Haj M, Waxsman I, Eitan A (2000) Evaluation of seprafilm and amniotic membrane as adhesion prophylaxis in mesh repair of abdominal wall hernia in rats. Eur Surg Res 32(2):125–128
22. Greenawalt KE, Butler TJ, Rowe EA, Finneral AC, Garlick DS, Burns JW (2000) Evaluation of sepramesh biosurgical composite in a rabbit hernia repair model. J Surg Res 94(2):92–98

23. Shapiro L, Holste JL, Muench T, diZerega G (2015) Rapid reperitonealization and wound healing in a preclinical model of abdominal trauma repair with a composite mesh. Int J Surg 22:86–91
24. Ar'Rajab A, Ahrén B, Rozga J, Bengmark S (1991) Phosphatidylcholine prevents postoperative peritoneal adhesions: an experimental study in the rat. J Surg Res 50(3):212–215
25. Holmdahl L, Risberg B, Beck DE, Burns JW, Chegini N, Di Zerega GS, Ellis H (1997) Adhesions: pathogenesis and prevention. Eur J Surg Suppl 577:56–62
26. Felemovicius I, Bonsack ME, Hegerman G, Delaney JP (2004) Prevention of adhesions to polypropylene mesh. J Am Coll Surg 198(4):543–548
27. Brochhausen C, Schmitt VH, Rajab TK, Planck CN, Krämer B, Tapprich C, Wallwiener M, Hierlemann H, Planck H, Kirkpatrick CJ (2012) Mesothelial morphology and organisation after peritoneal treatment with solid and liquid adhesion barriers—a scanning electron microscopical study. J Mater Sci Mater Med 23(8):1931–1939
28. Arnaud JP, Hennekinne-Mucci S, Pessaux P, Tuech JJ, Aube C (2003) Ultrasound detection of visceral adhesions after intraperitoneal ventral hernia treatment: a comparative study of protected versus unprotected meshes. Hernia 7(2):85–88
29. Balique JG, Benchetrit S, Bouillot JL, Flament JB, Gouillat C, Jarsaillon P, Lepère M, Mantion G, Arnaud JP, Magne E, Brunetti F (2005) Intraperitoneal treatment of incisional and umbilical hernias using an innovative composite mesh: four-year results of a prospective multicenter clinical trial. Hernia 9(1):68–74
30. Moreno-Egea A, Bustos JAC, Girela E, Aguayo-Albasini JL (2010) Long-term results of laparoscopic repair of incisional hernias using an intraperitoneal composite mesh. Surg Endosc 24(2):359–365
31. Chelala E, Debardemaeker Y, Elias B, Charara F, Dessily M, Alle JL (2010) Eighty-five redo surgeries after 733 laparoscopic treatments for ventral and incisional hernia: adhesion and recurrence analysis. Hernia 14(2):123–129
32. Celdrán A, García-Ureña MA, Bazire P, Marijuan JL (1996) The use of omentum in mesh repair of ventral hernias. Am Surg 62(6):443–445
33. Sorour MA (2014) Interposition of the omentum and/or the peritoneum in the emergency repair of large ventral hernias with polypropylene mesh. Int J Surg 12(6):578–586
34. Hasbahceci M, Basak F (2014) Interposition of the hernia sac as a protective layer in repair of giant incisional hernia with polypropylene mesh. Surg Today 44(2):227–232
35. D´Amore L, Ceci F, Mattia S, Fabbi M, Negro P, Gossetti F (2017) Adhesion prevention in ventral hernia repair: an experimental study comparing three lightweight porous meshes recommended for intraperitoneal use. Hernia 21(1):115–123

36. Boersema GS, Grotenhuis N, Bayon Y, Lange JF, BastiaansenJenniskens YM (2016) The effect of biomaterials used for tissue regeneration purposes on polarization of macrophages. Biores Open Access 5(1):6–14
37. Brown BN, Badylak SF (2013) Expanded applications, shifting paradigms and an improved understanding of host-biomaterial interactions. Acta Biomater 9(2):4948–4955
38. Sridharan R, Cavanagh B, Cameron AR, Kelly DJ, O'Brien FJ (2019) Material stiffness influences the polarization state, function and migration mode of macrophages. Acta Biomater 89:47–59
39. Grotenhuis N, Vd Toom HF, Kops N, Bayon Y, Deerenberg EB, Mulder IM, van Osch GJ, Lange JF, Bastiaansen-Jenniskens YM (2014) In vitro model to study the biomaterial-dependent reaction of macrophages in an inflammatory environment. BJS
101(8):983–992
40. Deeken CR, Matthews BD (2013) Characterization of the mechanical strength, resorption properties, and histologic characteristics of a fully absorbable material (poly-4-hydroxybutyrate-PHASIX Mesh) in a Porcine Model of hernia repair. ISRN Surg. https: //doi. org/10.1155/2013/23806 7
41. Martin DP, Badhwar A, Shah DV, Rizk S, Eldridge SN, Gagne DH, Ganatra A, Darois RE, Williams SF, Tai HC, Scott JR (2013) Characterization of poly-4-hydroxybutyrate mesh for hernia repair applications. J Surg Res 184(2):766–773
42. Scott JR, Deeken CR, Martindale RG, Rosen MJ (2016) Evaluation of a fully absorbable poly-4-hydroxybutyrate/absorbable barrier composite mesh in a porcine model of ventral hernia repair. Surg Endosc 30(9):3691–3701
43. Wolf MT, Dearth CL, Ranallo CA, LoPresti ST, Carey LE, Daly KA, Brown BN, Badylak SF (2014) Macrophage polarization in response to ECM coated polypropylene mesh. Biomaterials 35(25):6838–6849
44. Hong GS, Schwandt T, Stein K, Schneiker B, Kummer MP, Heneka MT, Kitamura K, Kalff JC, Wehner S (2015) Effects of macrophage-dependent peroxisome proliferator-activated receptor γ signalling on adhesion formation after abdominal surgery in an experimental model. Br J Surg 102(12):1506–1516